JACS
JOURNAL OF THE AMERICAN CHEMICAL SOCIETY
pubs.acs.org/JACS
Article

Nitrogen-Rich Tetrazolo[1,5-*b*]pyridazine: Promising Building Block for Advanced Energetic Materials

Wei Huang, Yongxing Tang,* Gregory H. Imler, Damon A. Parrish, and Jean'ne M. Shreeve*

Cite This: *J. Am. Chem. Soc.* 2020, 142, 3652–3657
Read Online
ACCESS | Metrics & More | Article Recommendations | Supporting Information

ABSTRACT: Two metal-free explosives, tetrazolo[1,5-*b*]pyridazine-containing molecules [6-azido-8-nitrotetrazolo[1,5-*b*]pyridazine-7-amine (**3at**) and 8-nitrotetrazolo[1,5-*b*]pyridazine-6,7-diamine (**6**)], were obtained via straightforward two-step synthetic routes from commercially available reagents. Compound **3at** displays an excellent detonation performance (D_v = 8746 m s^{-1} and P = 31.5 GPa) that is superior to commercial primary explosives such as lead azide and diazodinitrophenol (DDNP). Compound **6** has superior thermal stability, remarkable insensitivity, and good detonation performance, strongly suggesting it as an acceptable secondary explosive. The initiating ability of compound **3at** has been tested by detonating 500 mg of RDX with a surprisingly low minimum primary charge of 40 mg. The extraordinary initiating power surpasses conventional primary explosives, such as commercial DDNP (70 mg) and reported 6-nitro-7-azido-pyrazol[3,4-*d*][1,2,3]triazine-2-oxide (ICM-103) (60 mg). The outstanding detonation power of **3at** contributes to its future prospects as a promising green primary explosive. In addition, the environmentally benign methodology for the synthesis of **3at** effectively shortens the time from laboratory-scale research to practical applications.

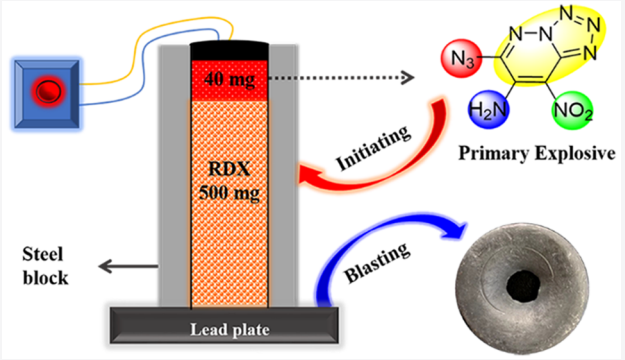

INTRODUCTION

To satisfy the growing demand for military and civilian applications, research concerning high energy density materials has attracted tremendous attention in the past decades. Mercury fulminate (MF), lead azide (LA), and lead styphnate (LS) have dominated the field of primary explosives for a very long time.[1] Because of the problems of long-term environmental contamination, health effects, and hazards from extreme sensitivities, it is essential to find green and efficient alternatives.[2] Considering the safety of operation and transportation, sensitivity to external stimuli is also a very important factor. Promising alternative materials should have properties such as powerful energetic performance, straightforward synthesis, good thermal stability, appropriate sensitivity, and high density and should be environmentally benign.[3]

Energetic organic materials are among the most promising replacements for LA and LS as green energetic materials[4] since they overcome the disadvantage of environmental hazards, while concomitantly providing high energetic performance.[5] Usually, in the initiation of an energetic material, the breaking of covalent bonds (C–N, N–N, or N–O) results in the rapid release of energy, leading to detonation.[6] As a result, designing materials based on nitrogen-rich heterocycles is an efficient strategy for the generation of novel energetic materials.[7] In recent years, a very large number of novel energetic materials based on nitrogen-rich heterocycles have been reported as insensitive powerful energetic materials.[8] The fused pyridazine-based group tetrazolo[1,5-*b*]pyridazine has been examined mainly as an active group in the synthesis of anti-inflammatory drugs.[9] It is noteworthy that the exceptionally high nitrogen content and high thermal stability could also give rise to materials with applications in energetic fields. However, tetrazolo[1,5-*b*]pyridazine has rarely been investigated as an energetic building block.[10]

Now novel energetic compounds were prepared based on tetrazolo[1,5-*b*]pyridazine by modifying the structure with different nitrogen-rich groups (nitro, amino, and azido). The two target molecules, 6-azido-8-nitrotetrazolo[1,5-*b*]-pyridazine-7-amine (**3at**) and 8-nitrotetrazolo[1,5-*b*]-pyridazine-6,7-diamine (**6**), were synthesized via facile and straightforward routes in high yields starting from commercially available 3,6-dichloropyridazin-4-amine. It is well known that practical applications of a large number of organic explosives are hindered due to multistep and low-yield synthetic routes.[11] Low-cost syntheses and easy scalability make **3at** and **6** valuable in real-world applications. The detonation performance, thermal stability, and moderate sensitivity of these novel materials surpass the performance

Received: January 9, 2020
Published: January 31, 2020

https://dx.doi.org/10.1021/jacs.0c00161
J. Am. Chem. Soc. 2020, 142, 3652–3657

Scheme 1. Synthesis of 3at

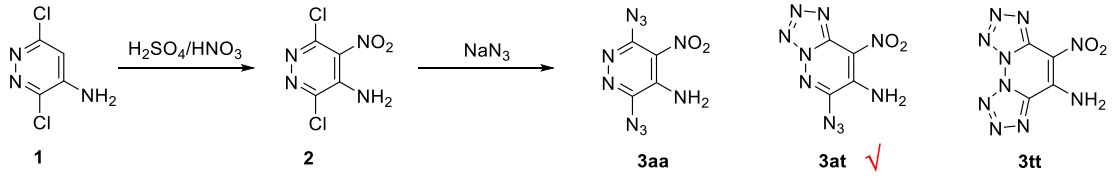

Scheme 2. Synthesis of 6

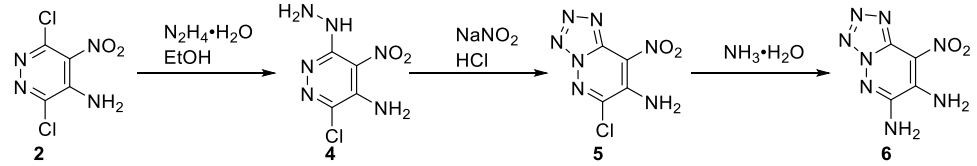

of some of the conventional explosives, suggesting great potential for practical applications.

RESULTS AND DISCUSSION

Synthesis. Compound **1** was nitrated with a mixture of 100% nitric acid and sulfuric acid to prepare **2**. Treatment of **2** with sodium azide in acetone/water resulted in the formation of **3at** (Scheme 1). Instead of a mixture of three tautomers [diazide (**3aa**), azide-tetrazole (**3at**), and ditetrazole (**3tt**)], the NMR spectra and single-crystal X-ray diffraction analysis support the sole existence of the azido-tetrazole form of **3at**. This phenomenon has been reported for a similar compound, 3,6-diazidopyridazine, where azido to tetrazolo tautomerism is possible, but it is found mainly in the tetrazole form.[12]

The synthetic route to **6** is shown in Scheme 2. Reaction of **2** with hydrazine monohydrate in ethanol gives the hydrazine-substituted compound **4**, which was treated with sodium nitrite in dilute HCl to yield the tetrazole-fused diazine compound **5**. Treatment of **5** with aqueous ammonia led to the formation of **6**, which was confirmed by single-crystal X-ray diffraction analysis. In addition, four 1,2,3-triazole *N*-oxide derivatives from **4** have also been prepared (Supporting Information). The related synthetic strategy has laid the groundwork for further preparative modification of pyridazine-fused energetic materials.

Crystal Structures. Suitable crystals of **3at** were obtained by evaporation of an acetone solution. It crystallizes in the monoclinic space group $P2_1/n$ with four formula moieties in the unit cell and a crystal density of 1.834 g cm^{-3} at 296 K. The molecular structure is given in Figure 1a. The molecule is planar with both of the torsion angles O(2)−N(3)−C(4)−C(5) and C(5)−C(7)−N(8)−N(9) at −179.9(2)°. As expected, the atoms (N8, N9, and N10) of the azido group are linear. The angle N(9)−N(8)−C(7) is 112.1(2)°. The intramolecular hydrogen bonding of N(6)−H(6A)···O(1) and intermolecular hydrogen bonding of N(6)−H(6B)···N(14)$^{\#}$ (symmetry code: $x-1, y, z$) form a three-dimensional network. Along the *a* axis, the layers are stacked by $\pi-\pi$ interactions and separated by distances of 2.673 and 3.037 Å, respectively.

Compound **6** also crystallizes in the monoclinic space group P21/n with four formula moieties in the unit cell with a DMSO molecule of crystallization. As shown in Figure 2, all the atoms in 6 are coplanar. The torsion angles for O(2)−N(3)−C(4)−C(14) and N(6)−C(5)−C(7)−N(8) are −1.2° and 1.1°, respectively. The bond lengths in 6 range from 1.295 Å (N11−N12) to 1.491 Å (C7−C5). The

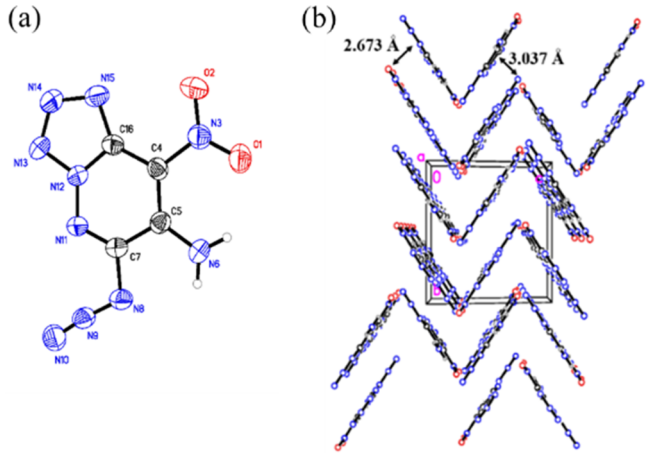

Figure 1. (a) Molecular structure of **3at**. (b) Packing diagram of **3at**.

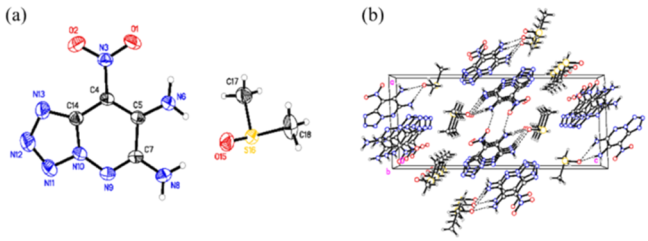

Figure 2. (a) Molecular structure of **6**. (b) Packing diagram of **6**.

bond angle for N9−N10−C14 is 129.8°. In addition, an intermolecular hydrogen bond, N(6)−H(6A)···O(1), is present, which aids in stabilizing the molecule.

Physical and Detonation Properties. Both **3at** and **6** are nitrogen-rich compounds, which makes them good candidates as energetic materials. Therefore, their physical and energetic properties were investigated. The thermal stability, detonation performance, and mechanical sensitivities are given in Table 1. The thermal decompositions of **3at** and **6** occur at onset temperatures of 163 and 290 °C, respectively. These values, especially for **6**, meet most military and civilian requirements. The drastic change in the thermal behavior from **3at** and **6** is a result of the replacement of the thermally sensitive azido group by a thermally stable amino group.

Due to the presence of a large number of N−N or C−N bonds, **3at** and **6** have a relatively high nitrogen content (**3at**: 63.66% and **6**: 57.90%). As a result, they have high positive

https://dx.doi.org/10.1021/jacs.0c00161
J. Am. Chem. Soc. 2020, 142, 3652−3657

Table 1. Physical and Detonation Properties of 3at and 6 in Comparison with LA, DDNP, and TATB

compound	T_d[a] [°C]	ρ[b] [g cm^{-3}]	$\Delta_f H$[c] [kJ mol^{-1}/kJ g^{-1}]	D_v[d] [m s^{-1}]	P[e] [GPa]	IS[f] [J]	FS[g] [N]
3at	163	1.82	811.2/3.65	8746	31.5	5	120
6	290	1.80	446.5/2.28	8434	27.7	>40	>360
LA[h]	315	4.80	450.1/1.55	5920	33.8	2.5−4	0.1−1
DDNP[i]	157	1.72	321.0/1.53	6900	24.7	1	24.7
TATB[j]	350	1.93	−139.7/-0.54	8179	30.5	50	>360

[a]Thermal decomposition temperature (onset) under nitrogen gas (DSC, 5 °C/min). [b]Measured densities, gas pycnometer at room temperature. [c]Calculated heat of formation. [d]Calculated detonation velocity. [e]Calculated detonation pressure. [f]Impact sensitivity. [g]Friction sensitivity; [h]Ref 3b. [i]Ref 14. [j]Ref 15.

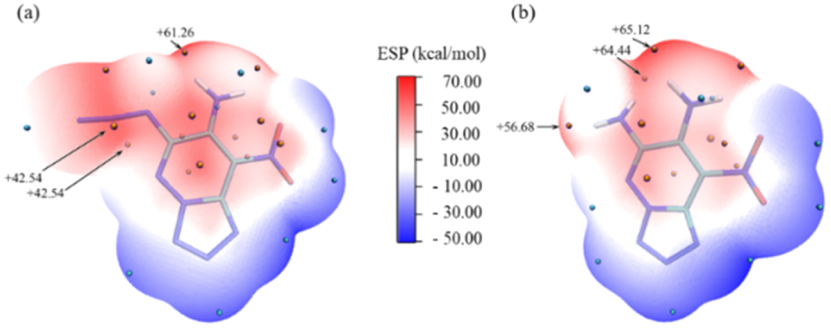

Figure 3. ESP-mapped molecular vdW surface of (a) **3at** and (b) **6**. Surface local minima and maxima of ESP are represented as blue and red spheres, respectively. Only the strong positive ESPs are labeled.

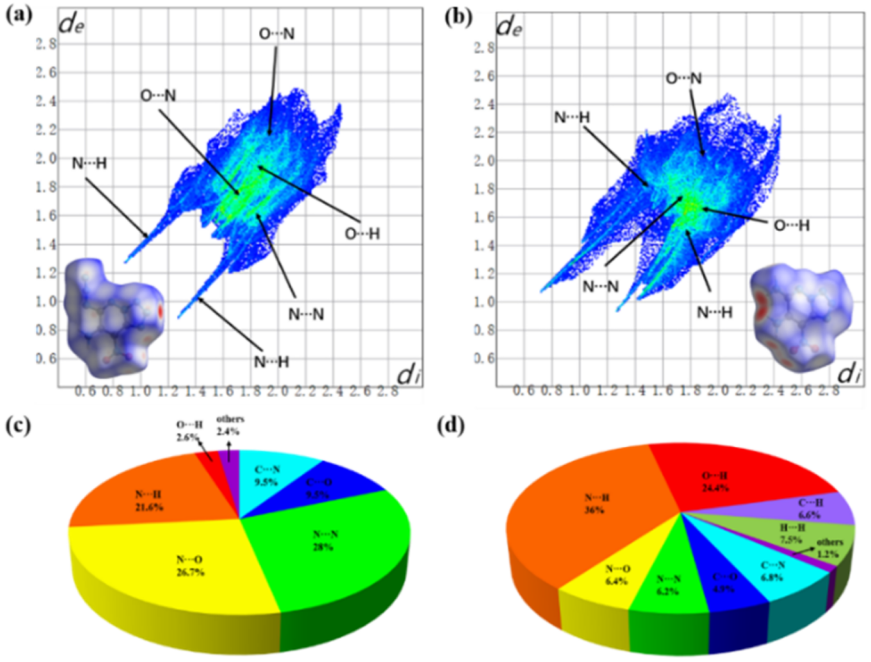

Figure 4. 2D fingerprint plots and Hirshfeld surfaces (inside) in crystal stacking for **3at** (a) and **6** (b); the pie graphs for **3at** (c) and **6** (d) show the percentage contributions of the individual atomic contacts to the Hirshfeld surface.

heats of formation (**3at**: 811.2 kJ mol^{-1}, 3.65 kJ g^{-1} and **6**: 446.5 kJ mol^{-1}, 2.28 kJ g^{-1}). This result is consistent with reports that the azido group increases the heat of formation by about +364 kJ mol^{-1}.[10a] The densities of **3at** and **6** were found to be 1.82 and 1.80 g cm^{-3}, respectively, by using a gas pycnometer at room temperature.

Detonation performances of **3at** and **6** were calculated by EXPLO5 software.[13] The values of detonation velocities (D_v) and pressures (P) are given in Table 1. Compound **3at** has an excellent detonation performance (D_v = 8746 m s^{-1} and P = 31.5 GPa), which is superior to commercial primary explosives, LA (D_v = 5920 m s^{-1} and P = 33.8 GPa)[3b] and DDNP (D_v = 6900 m s^{-1} and P = 24.7 GPa).[14] The sensitivities toward impact and friction were also determined. Compound **3at** has better safety and reliability than LA and DDNP, with impact (IS) and friction sensitivities (FS) of 5 J and 120 N, respectively. The relatively lower friction sensitivity should reduce the likelihood of accidents caused by slight amounts of friction. The moderate sensitivities nearly guarantee the possibility of the safety of production, handling, and trans-

https://dx.doi.org/10.1021/jacs.0c00161
J. Am. Chem. Soc. 2020, 142, 3652−3657

portation and retain competitive detonation performance at the same time. The good balance of detonation performance and sensitivity, plus the environmentally benign syntheses, contribute to the practical application of **3at** as a promising primary explosive. It is a green and powerful alternative to the toxic and sensitive LA.

Compound **6** not only has a very good detonation performance (D_v = 8434 m s^{-1} and P = 27.7 GPa) but also possesses remarkably low sensitivities, with IS > 40 J and FS > 360 N, which are comparable to the traditional insensitive explosive 2,4,6-triamino-1,3,5-trinitrobenzene (TATB) (IS = 50 J and FS > 360 N).[14] In addition, it has a desirable high thermal stability at T_d = 290 °C. The combined performance and properties of **6** suggest its potential as a secondary explosive for practical use.

The calculated electrostatic potentials (ESP) mapped vdW surfaces of **3at** and **6** are shown in Figure 3. In energetic compounds, the impact sensitivities of the molecules are closely related to their surface ESPs. Extensive areas with larger and stronger positive potentials usually result in increased impact sensitivities.[16] Compounds **3at** and **6** have similar electronegative areas (blue region). However, **3at** exhibits a notably larger electropositive area than **6**. Compound **3at** has anomalously strong positive potentials over its left portion, reflecting the depletion of electronic charge caused by the azido group. Therefore, compound **3at** is more sensitive than compound **6**, which is in accordance with the experimental results.

To gain additional insight in the relationship between sensitivity and structure, the Hirshfeld surface plots and two-dimensional fingerprint spectra of **3at** and **6** in the crystal structures were investigated and are shown in Figure 4. Both of the Hirshfeld surfaces of **3at** and **6** have nearly planar structures. The red dots appear in the side faces of the plates instead of the front faces, suggesting that the intermolecular interactions take place mainly through the external atoms (H, N, and O) encompassing the molecules. From the relative contribution of the contacts, the major interactions are N···N (28.0%), N···O (26.7%), and N···H (21.6%) for **3at** and N···H (36.0%), O···H (24.4%), and H···H (7.5%) for **6**. To sum up, the hydrogen-bridge contact is 24.2% (**3at**) and 67.9% (**6**), respectively. The remarkably abundant hydrogen bonds (67.9%) give rise to the low sensitivity of **6**.

Initiating Efficiency. The ability to initiate secondary explosives is one of the most important parameters for a primary explosive. To test the feasibility of **3at** as a primary explosive, an initiation capability test was performed by using it to detonate 500 mg of secondary explosive (RDX) against a 5 mm lead block (Figure 5a). To determine the minimum primary charge (MPC), a certain amount of **3at** was filled over 500 mg of RDX and pressed with a static pressure of 40 MPa. The apparatus was fired by an electric igniter. As is seen in Figure 5b, reducing the charge amount of **3at** from 80 mg to 40 mg has only a slight influence on the diameters of the blasted holes, which stay constant around 1.1 cm. Therefore, under a given charge of secondary explosive, the size of the blasted hole is independent of the charge of the primary explosive as long as it can initiate the process successfully. The test results demonstrate that **3at** is a super igniting explosive with an MPC of 40 mg, which is superior to that of the reported ICM-103 (60 mg)[2] and DDNP (70 mg).[14] Thus, **3at** is shown to have an extraordinary initiating ability and to demonstrate great promise for real applications. After many tests, **3at** has been demonstrated to be used in a detonator with an electric ignitor.

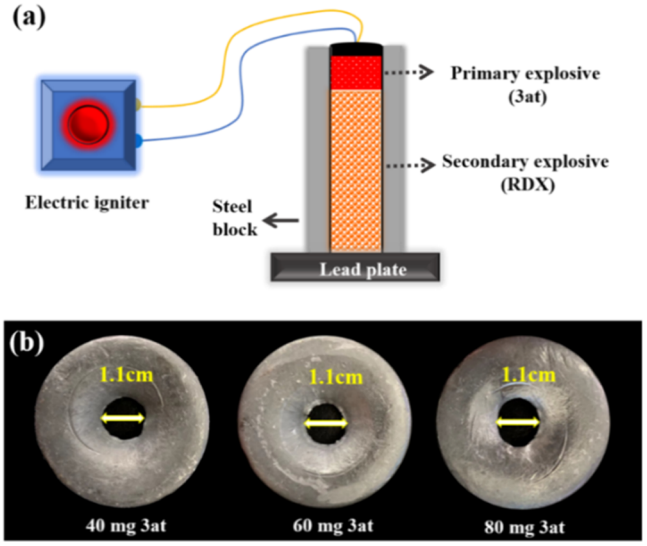

Figure 5. (a) Illustration of initiation capability test of **3at**. (b) Lead plates that were blasted out of the hole by using different amount of **3at** as primary explosive and 500 mg of RDX as secondary explosive.

In consideration of the good explosive performances of **3at** and **6**, the tetrazolo[1,5-*b*]pyridazine moiety appears to be an effective building block to construct highly energetic materials. With this experience, more powerful and insensitive energetics could be developed in future research.

■ CONCLUSION

In conclusion, two nitrogen-rich molecules (**3at** and **6**) based on tetrazolo[1,5-*b*]pyridazine were prepared from commercially available reagents by using straightforward synthetic methodology. The detonation performance and sensitivities toward mechanical stimuli were thoroughly examined. The prediction models, including ESP mapped surface, Hirshfeld surface, and related fingerprint plot analysis, were all examined to investigate the relationship between their structures and sensitivities. Compound **3at** displays a superior detonation performance (D_v = 8746 m s^{-1} and P = 31.5 GPa) compared to commercial primary explosives. Furthermore, in the detonation test, compound **3at** can detonate 500 mg of RDX successfully with an ultralow MPC of 40 mg, surpassing the commercial primary explosives (MPC: 70 mg for DDNP and 60 mg for ICM-103). The outstanding detonation power and environmentally benign methodology for the synthesis of **3at** contribute to its future prospects as an efficient green primary explosive. Compound **6** could possibly be a secondary explosive owing to its high thermal stability (T_d = 290 °C), remarkable insensitivity (IS > 40 J and FS > 360 N), and good calculated detonation performance (D_v = 8434 m s^{-1} and P = 27.7 GPa). The discoveries have led to a strategy for the design of lead-free environmentally friendly primary explosives and also introduce fresh perspectives and a new design of an organic explosive with super detonation performances.

■ EXPERIMENTAL DETAILS

Caution! *The compounds in this work are potentially energetic materials that could explode under certain conditions (e.g., impact, friction, or electric discharge), especially the azido compound* ***3at****. Appropriate safety precautions, such as the use of safety shields in a fume hood and personal*

https://dx.doi.org/10.1021/jacs.0c00161
J. Am. Chem. Soc. 2020, 142, 3652−3657

protection equipment (safety glasses, face shields, ear plugs, and gloves) should be taken at all times when handling these materials.

General Methods. All reagents were purchased from AKSci or Alfa Aesar in analytical grade and were used as supplied. The ^{1}H and ^{13}C spectra were recorded on a 300 MHz (Bruker AVANCE 300) nuclear magnetic resonance spectrometer. Chemical shifts for ^{1}H and ^{13}C NMR spectra are given with respect to external $(CH_3)_4Si$. [D_6]DMSO was used as a locking solvent unless otherwise stated. IR spectra were recorded using KBr pellets with an FT-IR spectrometer (Thermo Nicolet AVATAR 370). Density was determined at room temperature by employing a Micromeritics AccuPyc II 1340 gas pycnometer. Decomposition (onset) temperatures were recorded using a dry nitrogen gas purge and a heating rate of 5 °C min^{-1} on a differential scanning calorimeter (DSC, TA Instruments Q2000). Elemental analyses (C, H, N) were performed with a Vario Micro Cube Elementar Analyzer. Impact and friction sensitivity measurements were made using a standard BAM Fall hammer and a BAM friction tester.

Computational Methods. The gas phase enthalpies of formation were calculated based on isodesmic reactions. The enthalpy of reaction is obtained by combining the MP2/6-311++G** energy difference for the reactions, the scaled zero-point energies (ZPE), values of thermal correction (HT), and other thermal factors. The solid-state heats of formation were calculated with Trouton's rule according to eq 1 (T represents either the melting point or the decomposition temperature when no melting occurs prior to decomposition).[17]

$$\Delta H_{sub} = 188/\mathrm{J\ mol^{-1}\ K^{-1}} \times T \quad (1)$$

Crystal Structure Analysis. A clear brown block crystal (**3at**) of dimensions 0.063 × 0.041 × 0.033 mm^3 and a clear colorless block crystal (**6**·DMSO) of dimensions 0.196 × 0.090 × 0.040 mm^3 were mounted on a MiteGen MicroMesh using a small amount of Cargille immersion oil. Data were collected on a Bruker three-circle platform diffractometer equipped with a SMART APEX II CCD detector. The crystals were irradiated using graphite-monochromated Mo Kα radiation (λ = 0.710 73 Å). Data were collected at room temperature (20 °C).

Data collection was performed, and the unit cell was initially refined using APEX3 [v2015.5-2].[18] Data reduction was performed using SAINT [v8.34A][19] and XPREP [v2014/2].[20] Corrections were applied for Lorentz, polarization, and absorption effects using SADABS [v2014/2].[21] The structures were solved and refined with the aid of the program SHELXL-2014/7.[22] The full-matrix least-squares refinement on F^2 included atomic coordinates and anisotropic thermal parameters for all non-H atoms. Hydrogen atoms were located from the difference electron-density maps and added using a riding model.

*Synthesis of **3at**.* Compound **2** was synthesized from commercially available reagent **1** according to the literature.[23] Compound **2** (0.84 g, 4.0 mmol) was dissolved in a mixture of water (5 mL) and acetone (5 mL); then sodium azide (0.80 g, 12.31 mmol) was added. The reaction mixture was stirred for 12 h at room temperature. The precipitate was collected by filtration, washed with water, and dried in air (0.71 g, yield: 80%).

3at: brown solid. $T_{d\ (onset)}$: 163 °C. ^{1}H NMR (d_6-DMSO): 9.44 (s, 1H), 9.01 (s, 1H) ppm. ^{13}C NMR (d_6-DMSO): δ 149.1, 139.7, 138.1, 115.3 ppm. IR (KBr): $\tilde{\nu}$ = 3395, 3165, 2159, 1635, 1525, 1339, 1280, 1191, 1107, 1010, 988, 932, 775, 763, 724, 707, 648 cm^{-1}. $C_4H_2N_{10}O_2$ (222.13): calcd C 21.63, H 0.69, N 63.06%; found C 21.55, H 0.72, N 63.66%.

*Synthesis of **4**.* Hydrazine monohydrate (0.60 g, 12 mmol) in ethanol (5 mL) was added slowly to a solution of compound **2** (0.84 g, 4.0 mmol) in ethanol (20 mL) at 5 °C. The reaction mixture was stirred for 2 h, and the precipitate was collected by filtration, washed with ethanol (10 mL), and dried in air (0.72 g, yield: 88%).

4: orange solid. T_d (onset): 229 °C. ^{1}H NMR (d_6-DMSO): 9.20 (s, 1H), 8.43 (s, 2H), 4.90 (s, 2H) ppm. ^{13}C NMR (d_6-DMSO): δ 148.5, 141.0, 140.4, 116.5 ppm. IR (KBr): $\tilde{\nu}$ = 3434, 3339, 3104, 1638, 1577, 1490, 1436, 1317, 1271, 1175, 1076, 969, 881, 729, 720, 661 cm^{-1}. $C_4H_5ClN_6O_2$ (204.57): calcd C 23.48, H 2.46, N 41.08%; found C 23.52, H 2.55, N 41.68%.

*Synthesis of **5**·H_2O.* Compound **4** (0.56 g, 2.74 mmol) was dissolved in dilute HCl solution (12%, 12 mL), and a solution of sodium nitrite (0.22 g, 3.16 mmol) in water (2 mL) was added at 0 °C. The reaction mixture was stirred at 0 °C for 0.5 h. The precipitate was collected by filtration, washed with ice water (15 mL), and dried in air (0.48 g, yield: 75%).

***5**·H_2O:* white solid. T_m: 71 °C. $T_{d\ (onset)}$: 196 °C. ^{1}H NMR (d_6-DMSO): 9.67 (s, 1H), 9.32 (s, 1H) ppm. ^{13}C NMR (d_6-DMSO): δ 147.0, 141.4, 140.2, 115.9 ppm. IR (KBr): $\tilde{\nu}$ = 3404, 3182, 1636, 1576, 1542, 1519, 1450, 1352, 1318, 1282, 1203, 1161, 1097, 1062, 998, 982, 798, 773, 751, 727, 710, 685, 669 cm^{-1}. $C_4H_4ClN_7O_3$ (233.57): calcd C 20.57, H 1.73, N 41.98%; found C 20.58, H 1.81, N 42.46%.

*Synthesis of **6**.* Compound **5**·H_2O (0.46 g, 2.0 mmol) was suspended in acetonitrile (15 mL), and aqueous ammonia (28%, 2.0 g) was added. The autoclave (30 mL) was sealed, and the reaction mixture was heated to 95 °C and stirred for 10 h. After cooling, water (20 mL) was added and the reaction mixture was stirred for 0.5 h. The precipitate was collected by filtration, washed with water (20 mL), acetonitrile (10 mL), and diethyl ether (10 mL), and dried in air (0.31 g, yield: 78%).

6: yellow solid. $T_{d\ (onset)}$: 290 °C. ^{1}H NMR (d_6-DMSO): 7.38 (br) ppm. ^{13}C NMR (d_6-DMSO): δ 155.9, 145.6, 140.3, 109.9 ppm. IR (KBr): $\tilde{\nu}$ = 3349, 3219, 1686, 1634, 1574, 1548, 1429, 1397, 1359, 1277, 1252, 1191, 1113, 1019, 9999, 953, 937, 818, 772, 741, 644 cm^{-1}. $C_4H_4N_8O_2$(196.13): calcd C 24.50, H 2.06, N 57.13%; found C 24.82, H 2.13, N 57.90%.

■ ASSOCIATED CONTENT

Supporting Information

The Supporting Information is available free of charge at https://pubs.acs.org/doi/10.1021/jacs.0c00161.

Synthesis of 1,2,3-trizole *N*-oxide derivatives from **4**, crystal structures and analysis of the obtained compounds (PDF)

X-ray data (CIF)

X-ray data (CIF)

X-ray data (CIF)

X-ray data (CIF)

■ AUTHOR INFORMATION

Corresponding Authors

Yongxing Tang − *Nanjing University of Science and Technology, Nanjing 210094, China; Department of Chemistry, University of Idaho, Moscow, Idaho 83844-2343, United States;* orcid.org/0000-0002-9549-9195; Email: yongxing@uidaho.edu

Jean'ne M. Shreeve − *Department of Chemistry, University of Idaho, Moscow, Idaho 83844-2343, United States;* orcid.org/0000-0001-8622-4897; Email: jshreeve@uidaho.edu

Authors

Wei Huang − *Nanjing University of Science and Technology, Nanjing 210094, China*

Gregory H. Imler − *Naval Research Laboratory, Washington, D.C. 20375, United States;* orcid.org/0000-0002-9686-9186

Damon A. Parrish − *Naval Research Laboratory, Washington, D.C. 20375, United States*

Complete contact information is available at: https://pubs.acs.org/10.1021/jacs.0c00161

Notes

The authors declare no competing financial interest.

■ ACKNOWLEDGMENTS

Financial support of the Office of Naval Research (N00014-16-1-2089) and the Defense Threat Reduction Agency (HDTRA 1-15-1-0028) is gratefully acknowledged. This work was supported by the National Natural Science Foundation of China (No. 21905135), Province the Natural Science Foundation of Jiangsu Province (BK20190458), and the Fundamental Research Funds for the Central Universities (No. 30919011270).

■ REFERENCES

(1) (a) Wang, Q.; Han, J.; Zhang, Y.; Yan, Z.; Velasco, E.; Yang, L.; Wang, B.; Zang, S. Fabrication of Copper Azide Film through Metal-Organic Framework for Micro-Initiator Applications. *ACS Appl. Mater. Interfaces* **2019**, *11*, 8081−8088. (b) Fronabarger, J. W.; Williams, M. D.; Sanborn, W. B.; Bragg, J. G.; Parrish, D. A.; Bichay, M. DBX-1-A Lead Free Replacement for Lead Azide. *Propellants, Explos., Pyrotech.* **2011**, *36*, 541−550.

(2) Deng, M.; Feng, Y.; Zhang, W.; Qi, X.; Zhang, Q. A Green Metal-Free Fused-Ring Initiating Substance. *Nat. Commun.* **2019**, *10* (1−8), 1339.

(3) (a) Xu, J.; Sun, C.; Zhang, M.; Liu, B.; Li, X.; Lu, J.; Wang, S.; Zheng, F.; Guo, G. Coordination Polymerization of Metal Azides and Powerful Nitrogen-Rich Ligand toward Primary Explosives with Excellent Energetic Performances. *Chem. Mater.* **2017**, *29*, 9725−9733. (b) Fischer, D.; Klapötke, T. M.; Stierstorfer, J. Potassium 1,1′-dinitramino-5,5′-bistetrazolate: A Primary Explosive with Fast Detonation and High Initiation Power. *Angew. Chem., Int. Ed.* **2014**, *53*, 8172−8175. (c) Li, Y.; Qi, C.; Li, S.; Zhang, H.; Sun, C.; Yu, Y.; Pang, S. 1,1′-Azobis-1,2,3-triazole: A High-Nitrogen Compound with Stable N_8 Structure and Photochromism. *J. Am. Chem. Soc.* **2010**, *132*, 12172−12173.

(4) Huynh, M. H. V.; Hiskey, M. A.; Meyer, T. J.; Wetzler, M. Green Primaries: Environmentally Friendly Energetic Complexes. *Proc. Natl. Acad. Sci. U. S. A.* **2006**, *103*, 5409−5412.

(5) (a) Reichel, M.; Dosch, D.; Klapötke, T. M.; Karaghiosoff, K. Correlation between Structure and Energetic Properties of Three Nitroaromatic Compounds: Bis(2,4-dinitrophenyl) Ether, Bis(2,4,6-trinitrophenyl) Ether, and Bis(2,4,6-trinitrophenyl) Thioether. *J. Am. Chem. Soc.* **2019**, *141*, 19911−19916. (b) Liu, Y.; Zhao, G.; Tang, Y.; Zhang, J.; Hu, L.; Imler, G. H.; Parrish, D. A.; Shreeve, J. M. Multipurpose [1,2,4]triazolo[4,3-b][1,2,4,5] tetrazine-based Energetic Materials. *J. Mater. Chem. A* **2019**, *7*, 7875−7884. (c) Klapötke, T. M.; Stiasny, B.; Stierstorfer, J.; Winter, C. H. Energetic Organic Peroxides - Synthesis and Characterization of 1,4-Dimethyl-2,3,5,6-tetraoxabicyclo[2.2.1]heptanes. *Chem. Eur. Org. J.* **2015**, *21*, 6237−6242. (d) Klapötke, T. M.; Sabaté, C. M. Bistetrazoles: Nitrogen-Rich, High-Performing, Insensitive Energetic Compounds. *Chem. Mater.* **2008**, *20*, 3629−3637.

(6) Huynh, M. H. V.; Hiskey, M. A.; Chavez, D. E.; Naud, D. L.; Gilardi, R. D. Synthesis, Characterization, and Energetic Properties of Diazido Heteroaromatic High-Nitrogen C-N Compound. *J. Am. Chem. Soc.* **2005**, *127*, 12537−12543.

(7) (a) Herve, G.; Roussel, C.; Graindorge, H. Selective Preparation of 3,4,5-Trinitro-1H-pyrazole: A Stable All-Carbon-Nitrated Arene. *Angew. Chem., Int. Ed.* **2010**, *49*, 3177−3181. (b) Yin, P.; Zhang, J.; He, C.; Parrish, D. A.; Shreeve, J. M. Polynitro-substituted Pyrazoles and Triazoles as Potential Energetic Materials and Oxidizers. *J. Mater. Chem. A* **2014**, *2*, 3200−3208.

(8) (a) Dalinger, I. L.; Suponitsky, K. Y.; Shkineva, T. K.; Lempert, D. B.; Sheremetev, A. B. Bipyrazole Bearing Ten Nitro Groups - a Novel Highly Dense Oxidizer for Forward-Looking Rocket Propulsions. *J. Mater. Chem. A* **2018**, *6*, 14780−14786. (b) Tang, Y.; Dharavath, S.; Imler, G. H.; Parrish, D. A.; Shreeve, J. M. Nitramino- and Dinitromethyl-substituted 1,2,4-Triazole Derivatives as High-Performance Energetic Materials. *Chem. - Eur. J.* **2017**, *23*, 9185−9191. (c) Mikhailov, Y. M.; Chapyshev, S. V.; Nedel'ko, V. V. Synthesis, Thermal Stability, Heats of Formation, and Explosive Properties of Cyano-substituted Di-, Tri-, and Tetraazidopyridines. *Russ. Chem. Bull.* **2009**, *58*, 2097−2102.

(9) (a) Jose Lapponi, M.; Carestia, A.; Ines Landoni, V.; Rivadeneyra, L.; Etulain, J.; Negrotto, S.; Gabriel Pozner, R.; Schattner, M. Regulation of Neutrophil Extracellular Trap Formation by Anti-Inflammatory Drugs. *J. Pharmacol. Exp. Ther.* **2013**, *345*, 430−437. (b) Hafez, H. N.; Abbas, H. A. S.; El-Gazzar, A. R. B. A. Synthesis and Evaluation of Analgesic, Anti-Inflammatory and Ulcerogenic Activities of Some Triazolo- and 2-Pyrazolyl-pyrido [2,3-d]pyrimidines. *Acta Pharm.* **2008**, *58*, 359−378.

(10) Chen, S.; Liu, Y.; Feng, Y.; Yang, X.; Zhang, Q. 5,6-Fused Bicyclic Tetrazolo-Pyridazine Energetic Materials. *Chem. Commun.* **2020**, DOI: 10.1039/C9CC08782F.

(11) (a) Chen, D.; Yang, H.; Yi, Z.; Xiong, H.; Zhang, L.; Zhu, S.; Cheng, G. $C_8N_{26}H_4$: An Environmentally Friendly Primary Explosive with High Heat of Formation. *Angew. Chem., Int. Ed.* **2018**, *57*, 2081−2084. (b) Kumar, D.; Tang, Y.; He, C.; Imler, G. H.; Parrish, D. A.; Shreeve, J. M. Multipurpose Energetic Materials by Shuffling Nitro Groups on a 3,3′-Bipyrazole Moiety. *Chem. - Eur. J.* **2018**, *24*, 17220−17224.

(12) (a) Abdou, W. M.; Ganoub, N. A.; Sabry, E. Synthesis and Quantitative Structure-Activity Relationship Study of Substituted Imidazophosphor Ester Based Tetrazolo[1,5-b]pyridazines as Anti-nociceptive/Anti-Inflammatory Agents. *Beilstein J. Org. Chem.* **2013**, *9*, 1730−1736. (b) Kategaonkar, A. H.; Sapkal, S. B.; Madje, B. R.; Shingate, B. B.; Shingare, M. S. Synthesis of New 4-(4,5-Diphenyl-1H-imidazol-2-yl)tetrazolo[1,5-a]quinolines from Tetrazolo[1,5-a]-quinolines. *Chem. Heterocycl. Compd.* **2010**, *46*, 754−758.

(13) Súeska, M. *EXPLO5 6.01*; Brodarski Institute: Zagreb, Croatia, 2013.

(14) Fu, W.; Zhao, B.; Zhang, M.; Li, C.; Gao, H.; Zhang, J.; Zhou, Z. 3,4-Dinitro-1-(1H-tetrazol-5-yl)-1H-pyrazol-5-amine (HANTP) and Its Salts: Primary and Secondary Explosives. *J. Mater. Chem. A* **2017**, *5*, 5044−5054.

(15) Boddu, V. M.; Viswanath, D. S.; Ghosh, T. K.; Damavarapu, R. 2,4,6-Triamino-1,3,5-trinitrobenzene (TATB) and TATB-based Formulations-a Review. *J. Hazard. Mater.* **2010**, *181*, 1−8.

(16) (a) Baxter, A. F.; Martin, I.; Christe, K. O.; Haige, R. Formamidinium Nitroformate: An Insensitive RDX Alternative. *J. Am. Chem. Soc.* **2018**, *140*, 15089−15098. (b) Murray, J. S.; Concha, M. C.; Politzer, P. Links between Surface Electrostatic Potentials of Energetic Molecules, Impact Sensitivities and C-NO_2/N-NO_2 Bond Dissociation Energies. *Mol. Phys.* **2009**, *107*, 89−97.

(17) Westwell, M. S.; Searle, M. S.; Wales, D. J.; Williams, D. H. Empirical Correlations between Thermodynamic Properties and Intermolecular Forces. *J. Am. Chem. Soc.* **1995**, *117*, 5013−5015.

(18) Bruker. *APEX3* v2015.5-2; Bruker AXS Inc.: Madison, WI, USA, 2015.

(19) Bruker. *SAINT* v8.34A; Bruker AXS Inc.: Madison, WI, USA, 2013.

(20) Bruker. *XPREP* v2014/2; Bruker AXS Inc.: Madison, WI, USA, 2014.

(21) Bruker. *SADABS* v2014/5; Bruker AXS Inc.: Madison, WI, USA, 2014.

(22) Sheldrick, G. M. *SHELXL-2014/7*; University of Göttingen: Germany, 2014.

(23) Chmovzh, T.; Knyazeva, E.; Popov, V.; Rakitin, O. 4,7-Dichloro[1,2,5]oxadiazolo[3,4-d]pyridazine 1-oxide. *Molbank* **2018**, *2018* (1−3), 982.

https://dx.doi.org/10.1021/jacs.0c00161
J. Am. Chem. Soc. 2020, 142, 3652−3657